Salinibacter Sensory Rhodopsin
SENSORY RHODOPSIN I-LIKE PROTEIN FROM A EUBACTERIUM*

Tomomi Kitajima-Ihara[‡], **Yuji Furutani**[§], **Daisuke Suzuki**[‡], **Kunio Ihara**[¶], **Hideki Kandori**[§], **Michio Homma**[‡], **and Yuki Sudo**[‡1]

From the [‡]*Division of Biological Science, Graduate School of Science and the* [¶]*Center for Gene Research, Nagoya University, Chikusa-Ku, Nagoya, 464-8602, Japan and the* [§]*Department of Materials Science and Engineering, Nagoya Institute of Technology, Showa-ku, Nagoya, 466-8555, Japan*

Halobacterium salinarum **sensory rhodopsin I (**Hs**SRI), a dual receptor regulating both negative and positive phototaxis in haloarchaea, transmits light signals through changes in protein-protein interactions with its transducer, halobacterial transducer protein I (HtrI). Haloarchaea also have another sensor pigment, sensory rhodopsin II (SRII), which functions as a receptor regulating negative phototaxis. Compared with** Hs**SRI, the signal relay mechanism of SRII is well characterized because SRII from** Natronomonus pharaonis **(**Np**SRII) is much more stable than** Hs**SRI and** Hs**SRII, especially in dilute salt solutions and is much more resistant to detergents. Two genes encoding SRI homologs were identified from the genome sequence of the eubacterium** Salinibacter ruber**. Those sequences are distantly related to** Hs**SRI (~40% identity) and contain most of the amino acid residues identified as necessary for its function. To determine whether those genes encode functional protein(s), we cloned and expressed them in** Escherichia coli**. One of them (**Sr**SRI) was expressed well as a recombinant protein having all-**trans **retinal as a chromophore. UV-Vis, low-temperature UV-Vis, pH-titration, and flash photolysis experiments revealed that the photochemical properties of** Sr**SRI are similar to those of** Hs**SRI. In addition to the expression system, the high stability of** Sr**SRI makes it possible to prepare large amounts of protein and enables studies of mutant proteins that will allow new approaches to investigate the photosignaling process of SRI-HtrI.**

Microorganisms are subjected to a variety of environmental stimuli to which they respond and adapt. Sensory rhodopsin I (SRI),[2] a photoactive membrane-embedded retinylidene protein consisting of seven transmembrane helices, functions as a receptor regulating both negative and positive phototaxis in the archaeon *Halobacterium salinarum* (1, 2). The original state of SRI and its long-lived photointermediate (the M-intermediate) are important for positive and negative phototaxis, respectively, and have absorption maxima at 587 and 373 nm, respectively. Sensory rhodopsin II (SRII, also known as phoborhodopsin) is a negative phototaxis receptor in haloarchaea, including *H. salinarum* and *Natronomonas pharaonis*. Those are called *Hs*SRI and *Np*SRII, respectively, and their absorption maxima are at about 500 nm (3). Thus, haloarchaea are attracted to light with wavelengths longer than 520 nm, and they avoid light with wavelengths shorter than 520 nm because of the functions of SRI and SRII (2). Light >520 nm can activate the ion pumping rhodopsins, bacteriorhodopsin (BR), and halorhodopsin (HR), to obtain light energy, and cells avoid light of shorter wavelengths that contain harmful near-UV radiation (2).

*Hs*SRI and *Np*SRII form 2:2 signaling complexes with their cognate halobacterial transducer proteins (Htr), *Hs*HtrI and *Np*HtrII, in membranes, and transmit light signals through changes in protein-protein interactions (4). The excitation light absorbed by *Hs*SRI and *Np*SRII triggers *trans-cis* isomerization of the retinal chromophore that is covalently bound to a conserved lysine residue via a protonated Schiff base linkage (5, 6). This photoexcitation results in the sequential appearance of various photointermediates (K, L, M, and O) followed by a return to the unphotolyzed form of the protein (2, 7). The linear cyclic photochemical reaction is referred to as the photocycle.

In the dark (original) state of *Np*SRII, it has been reported that two specific hydrogen bonds between *Np*SRII and *Np*HtrII (8, 9), the deprotonation of Asp-193[*Np*SRII] (10) and the HAMP domain of *Np*HtrII (11), are important for their interactions. Upon formation of the K-intermediate, light activates the photoisomerization of retinal in *Np*SRII, which leads to steric constraint between Thr-204[*Np*SRII] and C14-H in the retinal chromophore (12, 13) and to alteration of the O-H stretching vibration of Thr-204 (14, 15), as revealed by phototaxis and FTIR experiments. Upon formation of the active M-intermediate, helix-F of *Np*SRII moves toward *Np*HtrII, as revealed by electron paramagnetic resonance spectroscopy (16) and chemical modification (17), which leads to helix rotation and/or helix movements of *Np*HtrII (18). At its distal end, activated *Np*HtrII binds a cytoplasmic histidine kinase, CheA. CheA phosphorylates a phosphoregulator (CheY) that binds to the flagellar motor switch and controls the swimming reversal probability of

[2] The abbreviations used are: SRI, sensory rhodopsin I; *Sr*SRI, *S. ruber* SRI; *Hs*SRI, *H. salinarum* SRI; *Np*SRII, *N. pharaonis* SRII (also known as *pharaonis* phoborhodopsin, *pp*R); HtrI, halobacterial transducer protein I; *Hs*HtrI, *H. salinarum* HtrI; *Sr*HtrI, *S. ruber* HtrI; *Np*HtrII, *N. pharaonis* HtrII; BR, bacteriorhodopsin; *Sr*SRI$_K$, *Sr*SRI K intermediate; *Sr*SRI$_M$, *Sr*SRI M intermediate; HPLC, high performance liquid chromatography; FTIR, Fourier transform infrared spectroscopy; MES, 4-morpholineethanesulfonic acid; MOPS, 4-morpholinepropanesulfonic acid; CHES, 2-(cyclohexylamino)ethanesulfonic acid; CAPS, 3-(cyclohexylamino)propanesulfonic acid.

the cell (19, 20). Thus, compared with *Hs*SRI, the signal relay mechanism of *Np*SRII is well characterized by various methods (21), because *Np*SRII is much more stable than *H. salinarum* SRII (22), especially in dilute salt solutions, and is much more resistant to detergents whereas *Hs*SRI is unstable under those conditions. Therefore, little is known about the molecular mechanism(s) of interactions between SRI and HtrI, about structural changes, or about the signal relay mechanism of positive phototaxis.

New genes encoding the sensory rhodopsin I-like protein have been recently discovered through genome sequencing of *S. ruber* (23). We present here the first characterization of SRI from the eubacterium *S. ruber* (*Sr*SRI). *Sr*SRI has all-*trans* retinal as a chromophore, has a longer absorption maximum (558 nm) than does SRII (500 nm), and has a slower photocycle than the light-driven ion-pumping rhodopsins (BR, HR, and proteorhodopsin), indicating similarities to the prototypic SRI (*Hs*SRI) (1). *Sr*SRI could be expressed in *Escherichia coli* and shows very high stability, even in detergent micelles, making it possible to prepare large amounts of protein. This also allows preparation of mutant *Sr*SRI, which will allow new approaches to investigate the photosignaling process in the SRI-HtrI system.

EXPERIMENTAL PROCEDURES

Plasmids and Strains—*S. ruber* (a kind gift from Dr. Dyall-Smith) was grown aerobically at 40 °C at pH 7.0 in medium with the following composition (g/liter): NaCl, 195; $MgSO_4 \cdot 7H_2O$, 25; $MgCl_2 \cdot 6H_2O$, 16.3; $CaCl_2 \cdot 2H_2O$, 1.25; KCl, 5.0; $NaHCO_3$, 0.25; NaBr, 0.625; and yeast extract (Difco), 1.0. Cells were harvested by centrifugation and were stored at −80 °C. Genomic DNA was prepared using the method of Marmur (24). *E. coli* DH5α was used as a host for DNA manipulation, and BL21(DE3) was used for expressing the genes. For DNA manipulation, the sensory rhodopsin I gene (SRU_2511) was amplified using PCR from the genomic DNA of *S. ruber*. The forward primer 5′- CATATGGACCCGATTACGATCGTCTA-3′ and the reverse primer 5′-CTCGAGGGCGGCAGACGTGACT-GTCGC-3′ were designed (underlining indicates the restriction sites for NdeI and XhoI, respectively). The stop codon was deleted during amplification. The NdeI and XhoI fragment was ligated to NdeI and XhoI sites of pET21c(+) vector (Novagen, Madison, WI). Consequently, the plasmid encodes six histidines at the C terminus, and it was named pTK001. This cloning strategy resulted in the following N- and C-terminal peptide sequences: [1]MDPI----TSAA[239]LEHHHHHH. The constructed plasmid was analyzed using an automated sequencer to confirm the expected nucleotide sequence. Another SRI gene, SRU_2579, was amplified and cloned using almost the same strategy as SRU_2511, except for the use of the restriction site NheI instead of NdeI.

Protein Expression, Purification, and Reconstitution into PG Liposomes—Cells were grown in LB medium supplemented with ampicillin (final concentration of 100 μg/ml). *E. coli* BL21(DE3) harboring pTK001 was grown to an A_{660} of 0.3–0.5 in a 30 °C incubator, followed by the addition of 0.5 mM isopropyl-1-thio-β-D-galactopyranoside and 10 μM all-*trans* retinal. Cells were harvested at 3-h postinduction by centrifugation at

4 °C, resuspended in buffer (50 mM MES, pH 6.5) containing 4 M NaCl, and disrupted by sonication. Cell debris was removed by a low speed centrifugation (5,000 × g, 10 min, 4 °C). For solubilization of the membranes, 1% (w/v) *n*-dodecyl-β-D-maltoside (DM) was added, and the suspension was incubated overnight at 4 °C. The solubilized membranes were isolated by high speed centrifugation (100,000 × g, 30 min, 4 °C), and the supernatant was incubated with Ni-nitrilotriacetic acid (NTA) superflow (Qiagen, Valencia, CA) for 30 min. Thereafter, the Ni-NTA resin was poured into a chromatography column and was washed extensively with buffer (50 mM MES, pH 6.0) containing 4 M NaCl, 20 mM imidazole, and 0.1% w/v DM to remove unspecifically bound proteins. The histidine-tagged proteins were then eluted with buffer (0.1% DM, 4 M NaCl, 50 mM MES, pH 6.0, 300 mM imidazole). The purified *Sr*SRI sample was then reconstituted into PG liposomes. For reconstitution of L-α-phosphatidylglycerol (Sigma) lipids, the lipids were dissolved in chloroform, and a thin lipid film on the wall of a flask was prepared by careful evaporation of the solvent. *Sr*SRI in buffer (0.1% DM, 1 M NaCl, 10 mM MES, pH 6.0, 100 mM imidazole) was added (at an *Sr*SRI:PG molar ratio of 1:50), and the suspension was gently stirred for 30 min at room temperature. Reconstitution by detergent removal was performed using Bio-Beads SM-2 (Bio-Rad), as previously described (25).

The expression plasmid of *Hs*SRI was constructed essentially as described previously (9). *Hs*SRI, with a tag of six histidines at the C-terminal end, was expressed in *E. coli* BL21(DE3). Preparation of crude membranes and purification of protein were done as described previously (25).

Room Temperature and Low Temperature UV-Vis Spectroscopy and HPLC Analysis—Room temperature UV-Vis spectra were obtained using a UV2400PC spectrophotometer with an ISR240A integrating sphere (Shimadzu, Kyoto, Japan). The PG-reconstituted sample was washed and resuspended in six buffers (citric acid, MES, HEPES, MOPS, CHES, and CAPS, whose concentrations were 10 mM each) with 1 M NaCl. The buffer composition had the same buffer capacity over a wide range of pH values (2–9). pH values of the sample suspensions were measured using an F-55 pH-meter with a 9669-C10 glass electrode (HORIBA, Kyoto, Japan).

Low-temperature UV-Vis spectra were measured using a V-550DS (JASCO, Tokyo, Japan) spectrophotometer with a cryostat (Optistat DN, Oxford, UK) and a temperature controller (ITC 502, Oxford, UK) with liquid nitrogen as the coolant, as described previously (26). The PG-reconstituted sample with 5 mM NaCl and 2 mM phosphate buffer (pH 7.0) was placed on a BaF_2 window, and then was dried to a film under reduced pressure with an aspirator. The films were hydrated with water. *Sr*SRI$_K$ minus *Sr*SRI difference spectra were measured at 77 K, as follows: Illumination of the *Sr*SRI film with >450 nm light for 2 min, after which at pH 7.0 and 77 K converted *Sr*SRI to *Sr*SRI$_K$, and subsequent illumination with >640 nm light for 1 min forced *Sr*SRI$_K$ to revert to *Sr*SRI. *Sr*SRI$_M$ minus *Sr*SRI difference spectra were measured at 200 K and pH 7.0 as follows: To convert *Sr*SRI to *Sr*SRI$_M$, the sample was irradiated with >480 nm light for 2 min, after which a subsequent 1-min illumination with UV light-changed *Sr*SRI$_M$ back to *Sr*SRI. The

difference spectrum was calculated from the spectra before and after the illumination.

High performance liquid chromatography (HPLC) analysis was performed as described previously (27). The PG-reconstituted sample was analyzed in buffer (1 M NaCl, 50 mM Tris-Cl, pH 7.0). The HPLC system consisted of a PU-2080 pump and a UV-2075 UV/Vis detector (JASCO). The chromatograph was equipped with a silica column (6.0 × 150 mm; YMC-Pack SIL), the solvent was 12% (v/v) ethyl acetate and 0.12% (v/v) ethanol in hexane, and the flow rate was 1.0 ml/min. Extraction of retinal oxime from the sample was carried out by hexane after denaturation by methanol and 500 mM hydroxylamine at 4 °C. The molar composition of retinal isomers was calculated from the areas of the peaks monitored at 360 nm. Assignment of each peak was performed by comparing it with the HPLC pattern from retinal oximes of authentic all-*trans*- and 13-*cis*-retinals. For the light-adapted *Sr*SRI, the sample was irradiated with >480 nm light for 1 min. Two independent measurements were averaged.

Time-resolved Laser Spectroscopy—The purified sample in DM detergent micelles was resuspended in 50 mM Tris-HCl, pH 7.0, 0.1% DM, and 1 M NaCl. Flash-induced absorption changes in the 300–700-nm region in the millisecond to second time window with a 10-ms interval were acquired using a commercial flash photolysis system (Hamamatsu Photonics K. K., Hamamatsu, Japan), which consisted of a CCD linear detector (Photonic Multichannel Spectral Analyzer PMA-11 C8808–01), a CW xenon lamp L8004 as a light source and a sample room (flash photolysis optics C9125). Excitation of the *Sr*SRI samples was done by 556-nm nanosecond laser pulses (FWHM; 3.5 nm) from a Nd-YAG laser apparatus (LS-2134UT-10; LOTIS TII: 355 nm, 7 ns, 60 mJ) through an Optical Parametric Oscillator (OPO) (LT-2214-OPO/PM; LOTIS TII). The repetition rate of the laser pulses was 10 Hz and was reduced to 0.5 Hz using a beam shutter unit (BD-10MN-OPO; LOTIS TII) and a frequency divider to wait for completion of the photocycle of *Sr*SRI. The energy of one laser pulse is 3.8 mJ. Synchronization of data acquisition and laser triggering was performed using a delay pulse generator (DG535; Stanford Research Systems, Location Sunnyvale, CA). For signal-to-noise improvement, twenty photoreactions were averaged for one time slice and 3 sets of time-resolved light-induced difference spectra were recorded and averaged for a sample solution (experiment length of ~6 h). Two experiments were performed and in all, 6 sets of transient spectra were averaged. The bleach of the sample was negligible (~5%) in each experiment. The temperature of the sample was kept at 20 °C by circulating water through a thermoregulated bath (NCB-1200; EYELA, Tokyo, Japan).

Protein Stability in Low Salt Conditions—Absorption spectra were obtained using a UV-2550 (Shimadzu) spectrometer. To monitor the effects of salt concentration on the absorbance of SRI, PG-reconstituted samples were resuspended in a buffer containing 50 mM Tris-Cl, pH 7.0. Samples were taken at different time intervals, and the absorption spectra were measured.

RESULTS AND DISCUSSION

Two Sensory Rhodopsin I-like Proteins in the Genome of S. ruber—The genome sequence of *S. ruber* contains two genes coding for sensory rhodopsin I (SRU_2511, which are named *Sr*SRI, and SRU_2579). To date, these are the only examples (other than sensory proteorhodopsin from γ-proteobacteria) of an SRI gene discovered outside the Archaea (28). However, the properties of sensory proteorhodopsin have not been identified yet, because it is not expressed in *E. coli*, *Pichia pastoris*, or *H. salinarum*. The sequences of SRU_2511(*Sr*SRI) and SRU_2579 are distantly related to *Hs*SRI (~40% identity) (29) and contain most of the amino acid residues (Asn-165, His-166, Asp-201, Arg-215) identified as necessary for function (30–33) (Fig. 1), except for the equivalent of Tyr-163 in SRU_2511. Fig. 1 shows the secondary structure of SRI-like proteins from *S. ruber*. It is well known that the sensory rhodopsins have seven transmembrane domains and that retinal is the chromophore. A lysine (Lys-205) and an aspartate residue (Asp-72), predicted to be necessary for stabilization of the Schiff base and for the binding between protein and retinal, are completely conserved among SRIs (Fig. 1). Unexpectedly, His-166, one of the most important residues for active site proton transfer and phototaxis signaling (31) in *Hs*SRI is replaced by Tyr in one of the sensory rhodopsin I-like proteins from *S. ruber* (SRU_2511). These genes, SRU_2511 and SRU_2579, which have a downstream sequence are immediately followed by the same second gene in a probable operon that is under the control of the same promoter as rhodopsin. These putative transducer genes (SRU_2510, Htr for SRU_2511, and SRU_2580, Htr for SRU_2579) encode a ~650-residue protein with two transmembrane domains at the N-terminal portion followed by an extensive domain with primarily hydrophilic residues. This topology is similar to that of the Htr transducers from the archaeon *H. salinarum* (34). The eubacterium, *S. ruber*, also has two light-driven ion pumps, Xanthorhodopsin and a Halorhodopsin-like protein, making an energy source for living cells (23, 35). The sensory rhodopsins would function as a positive phototaxis sensor against longer wavelengths of light (where ion pumping rhodopsins can utilize light energy) and as a negative phototaxis sensor against shorter wavelengths of light (which contains harmful UV).

Protein Expression, Purification, and Absorption Spectrum—To determine whether the genes encode functional proteins, we cloned and expressed the two sensory rhodopsins, SRU_2511 and SRU_2579, in *E. coli* BL21(DE3) cells. Using PCR, we obtained a fragment containing the full-length of the SRU_2511 and SRU_2579 gene coding regions. An NdeI site was created at the translation initiation site in the PCR product using an oligonucleotide primer containing the NdeI site. A XhoI site was created, and the stop codon was deleted during the amplification. The NdeI and XhoI fragment of the PCR product was cloned into the NdeI and XhoI sites of pET21c(+). Induction of *E. coli* BL21(DE3) with 0.5 mM isopropyl-1-thio-β-D-galactopyranoside caused growth inhibition, suggesting they expressed the desired protein. Actually, upon addition of retinal, a color change of the SRU_2511-transformed cells was recognized, and the color was definitely distinct from cells
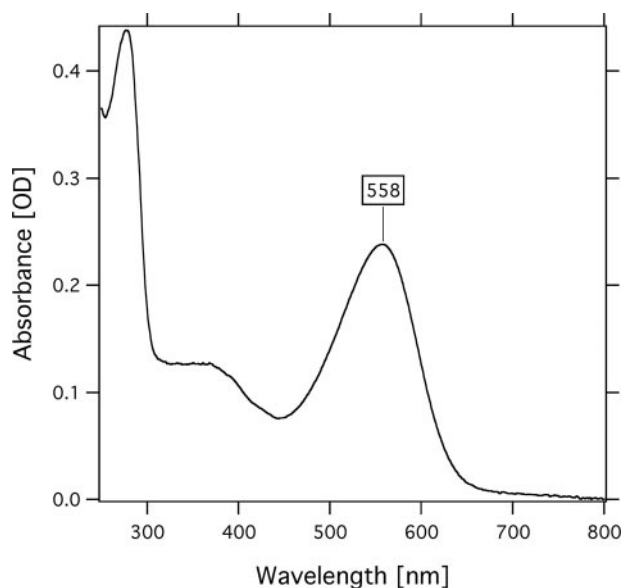
FIGURE 2. **The absorption spectrum of *Sr*SRI.** The protein was reconstituted into PG liposomes and was resuspended in buffer solution (50 mM Tris-HCl, pH 7.0, 1 M NaCl). The temperature was kept at 20 °C.

FIGURE 3. **Chromophore configuration extracted from *Sr*SRI reconstituted into PG liposomes with 1 M NaCl and 50 mM Tris-Cl (pH 7. 0).** The detection beam was set at 360 nm. Ts, Ta, 13s, and 13a stand for all-*trans* 15-*syn* retinal oxime, all-*trans* 15-*anti* retinal oxime, 13-*cis* 15-*syn* retinal oxime, and 13-*cis* 15-*anti* retinal oxime, respectively. The molar composition of retinal isomers was calculated from the areas of the peaks in the HPLC patterns. The chromophore configuration extracted from *Sr*SRI suspended in buffer solution containing 0.1% DM is given in *parentheses*.

transformed only by the vector pET21c(+), whereas cells containing SRU_2579 did not show any visible color, implying it was not expressed in the *E. coli* cells. SRU_2511 is hereafter called *Sr*SRI. Purified *Sr*SRI was reconstituted into PG liposomes, and the absorption spectrum was obtained as shown in Fig. 2. The absorption maximum of *Sr*SRI is located at 558 nm. That maximum wavelength is similar to that of *Hs*SRI (587 nm) (1) and is significantly different from the sensory rhodopsin II whose maximum is located at around 500 nm (36, 37). Thus, we were able to express a sensory rhodopsin I-like protein as a photoactive protein.

Retinal Configuration and pK_a of the Counterion—To investigate the physical properties of *Sr*SRI, HPLC analysis and pH-titration experiments were carried out. In the dark, light-driven ion pumps (BR and HR) use all-*trans* and 13-*cis* retinal (38, 39), whereas the photosensors *Hs*SRI, *Hs*SRII, and *Np*SRII use only all-*trans* retinal (40, 41). Fig. 3 shows the retinal isomer composition. The isomeric state of retinal is predominantly all-*trans*, with a small proportion of 13-*cis*, indicating that the retinal composition is markedly sensory rhodopsin-like. In all retinal proteins (except for Halorhodopsins), the protonated Schiff base is stabilized by an aspartic acid as a counterion. Spectroscopic pH-titration was performed to estimate the pK_a value of the counterion of *Sr*SRI (Asp-72) in the unphotolyzed state because protonation of Asp-72 causes a red-shift at the absorption maximum (see Fig. 4a). Fig. 4b shows that difference absorption spectra. Each spectrum obtained by subtracting that of pH 8.5. The different spectra clearly showed that the acid form has 2-fold larger extinction coefficient than the alkaline form as well as *Hs*SRI (42). The titration curves were analyzed
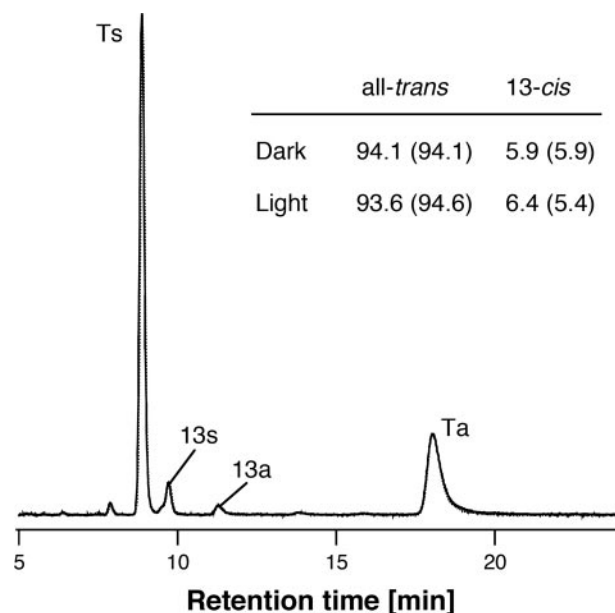
using the Henderson-Hasselbalch equation with a single pK_a value (43) (Fig. 4c). The pK_a value of Asp-72 for the PG-reconstituted *Sr*SRI was 4.3, which is 3 units lower than that of *Hs*SRI (~7.2) (44), suggesting a structural difference around the chromophore between *Sr*SRI and *Hs*SRI. Although the pK_a value of *Sr*SRI might be affected by interaction with *Sr*HtrI because the value of *Hs*SRI is elevated to 8.5 upon *Hs*HtrI association (44), the lower pK_a of *Sr*SRI also indicates that Asp-72 exists in a deprotonated form at neutral pH where the bacteria exist, suggesting the functional importance of the deprotonated state of *Sr*SRI.

Photocycle of SrSRI as Revealed by Time-resolved Flash Photolysis and Low Temperature UV-Vis Spectroscopy—To confirm the photocycle of *Sr*SRI, flash photolysis and low temperature UV-Vis spectroscopy were used (Figs. 5 and 6), and a schematic drawing of the photocycle based on the results is shown in Fig. 7. The *upper panel* in Fig. 5 shows the flash-induced difference spectrum of DM-solubilized *Sr*SRI over the spectral range from 300 to 700 nm. In this experiment, the *Sr*SRI sample contained 0.1% DM as a detergent to increase the S/N ratio without inactivation. Depletion by the flash and recovery of the original pigment was observed at 557 nm. The value was almost the same as the absorption maximum of *Sr*SRI shown in Fig. 2 (558 nm). At 390 nm, an increase and a decrease of absorbance were observed, implying the formation and decay

FIGURE 1. *a*, secondary structure of *S. ruber* sensory rhodopsin I (*Sr*SRI, SRU_2511). *b*, alignment of putative amino acid sequences of SRIs reported so far (29) with *Sr*SRI. Names of archaeal and bacterial sensory rhodopsins and sources from top are: cso_Hva, *Haloarcula vallismortis* cruxsensory rhodopsin (GenBank™ code: D83748); sop-F5R, *H. salinarum* strain Flx5R sR (L05603); sop-SGI, *Hb.* sp. strain SGI sR (X70290); SRU_2511, *S. ruber* strain DSM 13855 (3852586); SRU_2579, *S. ruber* strain DSM 13855 (3852268). Amino acid residues marked by an *asterisk* in helices F and G are important residues for phototaxis in SRI. The amino acid residues identified as necessary for function (31) were conserved among them except for a His residue (His-166 in *Hs*SRI).
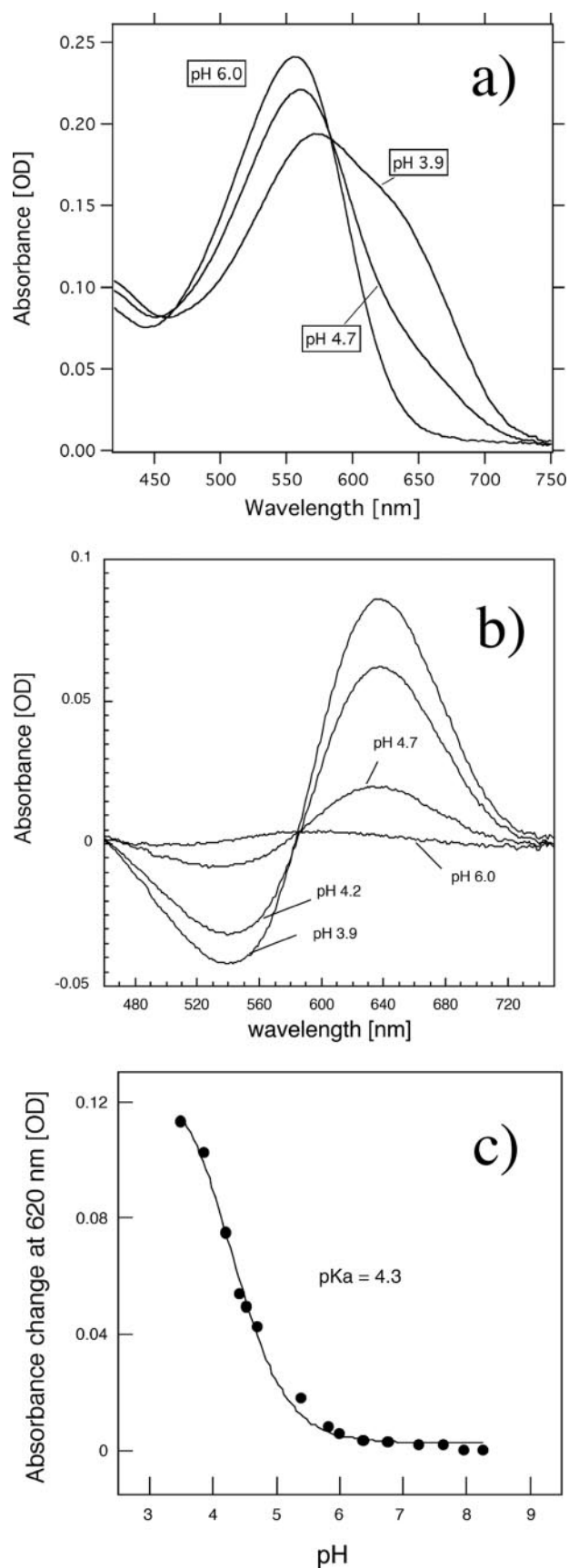
FIGURE 4. *a*, absorption spectrum of PG-reconstituted *Sr*SRI at pH 6. 0, 4.7, and 3.9. *b*, difference absorption spectra. Each spectrum was obtained by subtracting that of pH 8.5. *c*, pH-titration curves of the counterion, Asp-72, in
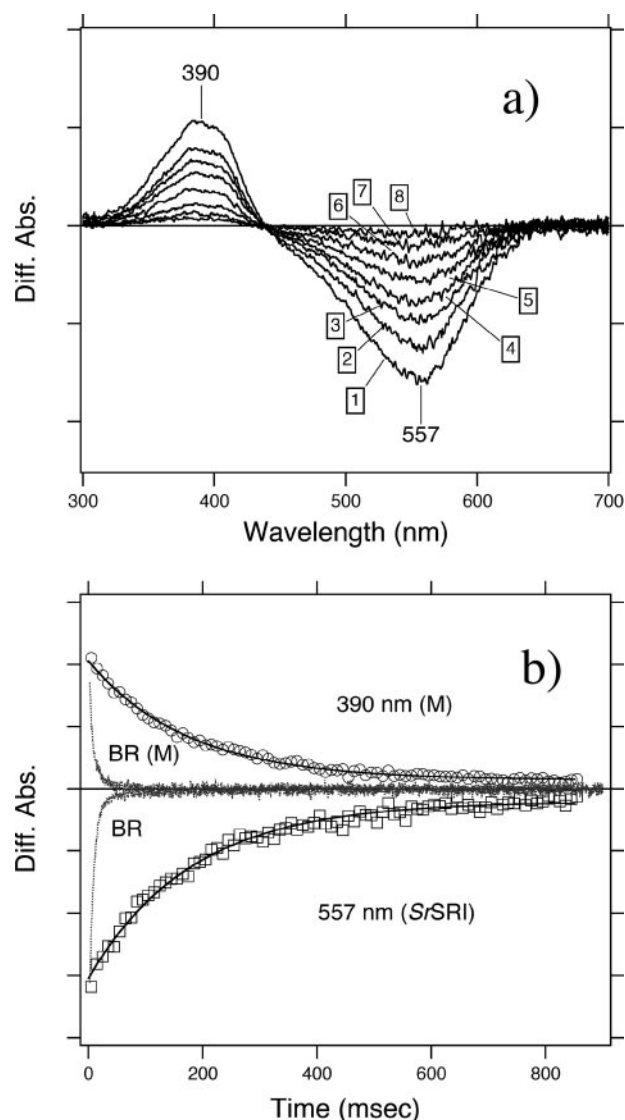
FIGURE 5. *a*, flash-induced difference spectra of DM-solubilized *Sr*SRI over a spectral range from 300 to 700 nm. The purified *Sr*SRI was resuspended in 50 mM Tris-HCl, pH 7.0, 0.1% DM, and 1 M NaCl. *Curves 1–8* are spectra of 10 ms (*1*), 50 ms (*2*), 90 ms (*3*), 130 ms (*4*), 210 ms (*5*), 330 ms (*6*), 540 ms (*7*), and 860 ms (*8*) after the illumination. The temperature was kept at 25 °C. *b*, flash-induced kinetic data of *Sr*SRI at 390 nm representing the M-decay and at 556 nm representing the recovery of the original *Sr*SRI. The kinetic data of BR were reproduced from Ref. (47) to compare the time range with *Sr*SRI. For BR, the M-intermediate and the unphotolyzed state were monitored at 410 and 570 nm, respectively.

of an intermediate $Sr\text{SRI}_M$ similar to $Hs\text{SRI}_M$ (S373) where an absorbance maximum is located at 373 nm. The *lower panel* in Fig. 5 shows the time courses of the absorbance change at selected wavelengths (390 nm for the M state and 557 nm for the unphotolyzed state). The M-decay rate is estimated as 6 s^{-1} by single exponential equation, close to that of *Hs*SRI (0.8 s^{-1}) (2) and of *Np*SRII (0.56 s^{-1}) (45). This slow photocycle is particularly important because a key difference between transport and sensory rhodopsins is the much slower kinetics of the photochemical reaction cycle of the sensors (46). The ion-pumping

*Sr*SRI. The *Sr*SRI sample was suspended in a mixture of six buffers with 1 M NaCl. The titration curves were analyzed using the Henderson-Hasselbalch equation with a single pK_a value (43). The temperature was kept at 20 °C.

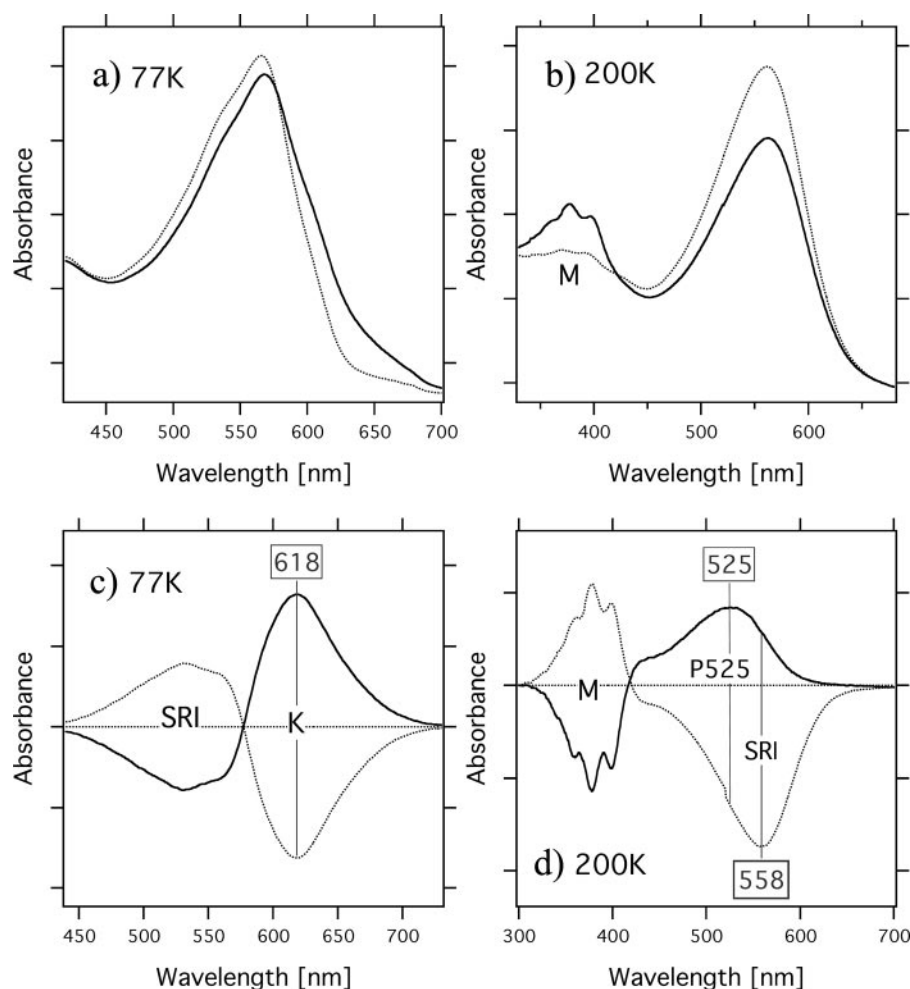FIGURE 6. **Low temperature UV-Vis absorption spectra of light-activated *Sr*SRI (*solid lines*) and *Sr*SRI in the dark (*dotted lines*) measured at 77 K (*a*) and at 200 K (*b*).** The protein was reconstituted into PG liposomes with NaCl. The difference spectra shown in *c* and *d*, were calculated from the spectra recorded before and after irradiation with light. One division of the *y*-axis of *a*, *b*, *c*, and *d* corresponds to 0.1, 0.1, 0.05, and 0.05 absorbance unit, respectively.

of the most important intermediates for the function of retinal proteins, except for HR. Low temperature FTIR and UV-Vis spectroscopy showed the formation of a small amount of an L-like intermediate of *Sr*SRI as judged by the absorption maximum and by the changes of C=C stretching vibration (data not shown), suggesting the presence of an L-intermediate in *Sr*SRI. In *Hs*SRI as well, K, L, and M intermediates appeared during the photocycle as they do in *Np*SRII (2, 7). The two difference spectra (dark minus light and light minus subsequent 1-min light illumination) in Fig. 6*c* are mirror images of each other, indicating that the K intermediates are photoreversible intermediates. However, the two difference spectra (dark minus light and light minus subsequent 1-min light illumination) in Fig. 6*d* are not mirror images of each other. Upon accumulation of *Sr*SRI$_M$ (Fig. 6*d*, *solid line*), the *Sr*SRI$_M$ forms a P510-like blue-shifted intermediate (P525), which is important for negative phototaxis in *Hs*SRI (1), and the P525 was also trapped at the temperature region between 170 and 243 K. In *Hs*SRI, the M intermediate (S373) becomes the P510-intermediate by illumination with UV light (1). We confirmed that the P510-intermediate of *Hs*SRI is also accumulated in our condition. The identified photocycle scheme is described in Fig. 7.

rhodopsins (BR, HR, and proteorhodopsin) have been optimized for fast photocycling rates to make them efficient pumps (see the *gray line* in Fig. 5*b* and Ref. 47). In contrast, the sensory rhodopsins *Hs*SRI and *Np*SRII have slow photocycles (2, 45), which allows the transient accumulation of long-lived signaling states of the receptors to catalyze a sustained phosphorylation cascade controlling flagellar motor rotation. The slow photocycle of *Sr*SRI therefore is a similar property to that of sensory rhodopsins from other sources.

Fig. 6 shows low temperature UV-Vis absorption spectra of light-activated *Sr*SRI (*solid lines*) and *Sr*SRI in the dark (*dotted lines*) measured at 77 K (*a*) and at 200K (*b*). The difference spectra shown in the panels (*c* and *d*) were calculated from the spectra recorded before and after irradiation with light. At 77 K, a light-induced spectral red shift was observed, implying the formation of a K-intermediate of *Sr*SRI. The formation of a K-intermediate was also confirmed by FTIR spectroscopy.[3] At 200 K, a spectral blue shift was observed, implying the formation of the M-intermediate of *Sr*SRI. The M-intermediate is one

Protein Stability of SrSRI—In 1982, using a BR mutant from the archaeon *H. salinarum* that was believed to express only HR at that time, Tsuda *et al.* (48) and Hazemoto *et al.* (49), found two independent fast and slow photocycles. Bogomolni and Spudich (50) proposed that the pigment having the slow photocycle is the receptor for phototaxis in this bacterium, and they proved their hypothesis by flash photolysis of a mutant lacking both BR and HR, which showed almost the same level of phototaxis as that of the wild type (51). They named this retinal pigment protein sensory rhodopsin I (SRI). Of interest, the ground state of SRI functions as a sensor for positive phototaxis whose action maximum is located at ~580 nm, while the long-lived photointermediate absorbing maximally at 377 nm works as sensor for negative phototaxis (1). The signal relay mechanism from SR receptors to their cognate Htr transducers has become a focus of interest, in part because of its importance to the general understanding of communication between integral membrane proteins, about which little is known. Important advances in understanding the molecular mechanism of nega-
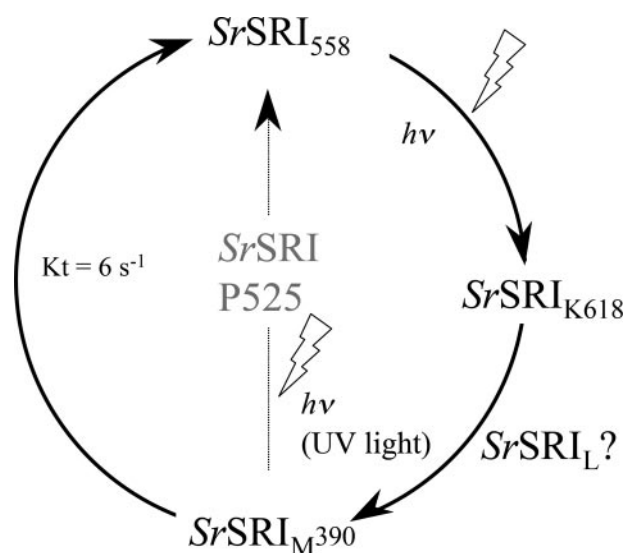
---

[3] Y. Sudo, unpublished data.

FIGURE 7. **Schematic of the photochemical reaction cycle of *Sr*SRI identified in this study.** hυ indicates light-dependent reactions, and the other *arrows* represent thermal reactions. The decay rate constant of *Sr*SRI$_M$ (6 s^{-1}) was obtained by a single exponential equation by the flash photolysis experiments shown in Fig. 5. *Hs*SRI absorbs orange light and forms the long-lived S373 intermediate, which forms the P510 intermediate upon the second photon absorption in the near-UV region (2).
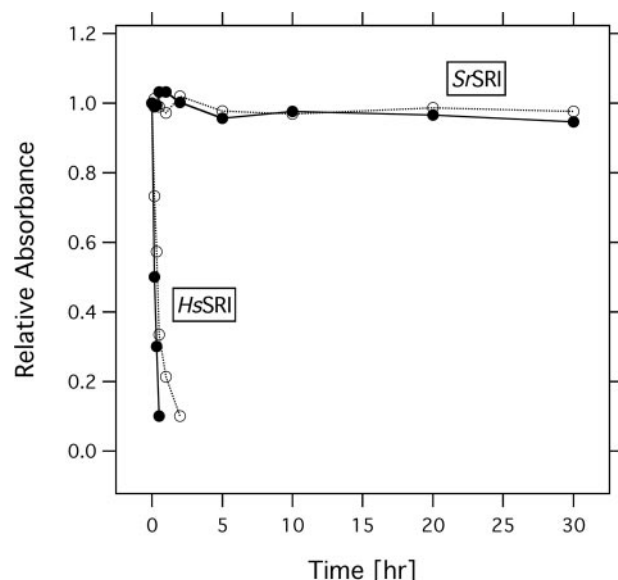

FIGURE 8. **Stability of *Hs*SRI and *Sr*SRI in the absence of NaCl (*solid lines*) and 50 mM NaCl (*dotted lines*).** The time-dependent absorbances of the proteins were plotted. The samples were reconstituted into PG-liposomes and resuspended in a buffer containing 50 mM Tris-Cl (pH 7.0), and the temperature was maintained at 20 °C.

tive phototaxis regulated by the SRII-HtrII complex has been made in recent years because *Np*SRII is much more stable than *Hs*SRI, especially in dilute salt solutions. Therefore, little is known about the molecular mechanism for positive phototaxis. In fact, the high-resolution crystal structures of BR, HR, and SRII and the SRII-HtrII complex were reported from 1997 through 2006 (52–56), whereas the structure of SRI has not been determined yet. Fig. 8 shows the protein stabilities of *Hs*SRI and *Sr*SRI under low salt conditions (0 and 50 mM NaCl) as judged by the absorbance of the proteins. A time-dependent decrease in the absorbance of *Hs*SRI was observed, implying the

degeneration of the protein within 5 h, whereas *Sr*SRI maintained its spectral stability over the 24 h (Fig. 8). As described in the pH-titration experiment, *Sr*SRI is also stable over a wide pH range (pH 3.5– 8.5) (Fig. 4). In addition, PG-reconstituted *Sr*SRI is stable even in the absence of NaCl, over a wide pH range (pH 2.5–10) and at high temperature (~60 °C) (data not shown), while *Hs*SRI is not stable under those conditions. Thus, *Sr*SRI expressed in *E. coli* shows high stability, making it possible to prepare large amounts of protein and enabling the study of mutant proteins, which will open new avenues to investigate the photosignaling process in the SRI-HtrI system. In the future, we will examine whether *Sr*SRI and *Sr*HtrI are expressed in native cells, and whether they regulate positive and/or negative phototaxis.

Concluding Remarks—In this study, we present the first characterization of SRI from a eubacterium *S. ruber*. The *Sr*SRI was expressed well (5 mg/liter culture) as a recombinant protein having all-*trans* retinal as a chromophore, and it is much more stable than SRI from the archaeon *H. salinarum* (*Hs*SRI) under various conditions. UV-Vis, low-temperature UV-Vis, pH-titration, and flash photolysis experiments revealed that the photochemical properties of *Sr*SRI are similar to those of SRI from the archaeon *H. salinarum*. In the future, we will examine whether *Sr*SRI and *Sr*HtrI regulate positive and/or negative phototaxis.

REFERENCES

1. Spudich, J. L., and Bogomolni, R. A. (1984) *Nature* **312,** 509–513
2. Hoff, W. D., Jung, K. H., and Spudich, J. L. (1997) *Annu. Rev. Biophys. Biomol. Struct.* **26,** 223–258
3. Sasaki, J., and Spudich, J. L. (2008) *Photochem. Photobiol.,* in press
4. Sasaki, J., Nara, T., Spudich, E. N., and Spudich, J. L. (2007) *Mol. Microbiol.* **66,** 1321–1330
5. Yan, B., Takahashi, T., Johnson, R., Derguini, F., Nakanishi, K., and Spudich, J. L. (1990) *Biophys. J.* **57,** 807–814
6. Kandori, H., Tomioka, H., and Sasabe, H. (2002) *J. Phys. Chem. A* **106,** 2091–2095
7. Chizhov, I., Schmies, G., Seidel, R., Sydor, J. R., Luttenberg, B., and Engelhard, M. (1998) *Biophys. J.* **75,** 999–1009
8. Hippler-Mreyen, S., Klare, J. P., Wegener, A. A., Seidel, R., Herrmann, C., Schmies, G., Nagel, G., Bamberg, E., and Engelhard, M. (2003) *J. Mol. Biol.* **330,** 1203–1213
9. Sudo, Y., Yamabi, M., Kato, S., Hasegawa, C., Iwamoto, M., Shimono, K., and Kamo, N. (2006) *J. Mol. Biol.* **357,** 1274–1282
10. Sudo, Y., Iwamoto, M., Shimono, K., and Kamo, N. (2004) *Biochemistry* **43,** 13748–13754
11. Sudo, Y., Okuda, H., Yamabi, M., Fukuzaki, Y., Mishima, M., Kamo, N., and Kojima, C. (2005) *Biochemistry* **44,** 6144–6152
12. Sudo, Y., Furutani, Y., Wada, A., Ito, M., Kamo, N., and Kandori, H. (2005) *J. Am. Chem. Soc.* **127,** 16036–16037
13. Sudo, Y., Furutani, Y., Spudich, J. L., and Kandori, H. (2007) *J. Biol. Chem.* **282,** 15550–15558
14. Sudo, Y., Furutani, Y., Shimono, K., Kamo, N., and Kandori, H. (2003) *Biochemistry* **42,** 14166–14172
15. Sudo, Y., Furutani, Y., Kandori, H., and Spudich, J. L. (2006) *J. Biol. Chem.* **281,** 34239–34245
16. Wegener, A. A., Chizhov, I., Engelhard, M., and Steinhoff, H. J. (2000) *J.*

Mol. Biol. **301,** 881–891

17. Yoshida, H., Sudo, Y., Shimono, K., Iwamoto, M., and Kamo, N. (2004) *Photochem. Photobiol. Sci.* **3,** 537–542

18. Wegener, A. A., Klare, J. P., Engelhard, M., and Steinhoff, H. J. (2001) *EMBO J.* **20,** 5312–5319

19. Rudolph, J., Tolliday, N., Schmitt, C., Schuster, S. C., and Oesterhelt, D. (1995) *EMBO J.* **14,** 4249–4257

20. Trivedi, V. D., and Spudich, J. L. (2003) *Biochemistry* **42,** 13887–13892

21. Spudich, J. L., and Luecke, H. (2002) *Curr. Opin. Struct. Biol.* **12,** 540–546

22. Sudo, Y., Yamabi, M., Iwamoto, M., Shimono, K., and Kamo, N. (2003) *Photochem. Photobiol.* **78,** 511–516

23. Mongodin, E. F., Nelson, K. E., Daugherty, S., Deboy, R. T., Wister, J., Khouri, H., Weidman, J., Walsh, D. A., Papke, R. T., Sanchez Perez, G., Sharma, A. K., Nesbo, C. L., MacLeod, D., Bapteste, E., Doolittle, W. F., Charlebois, R. L., Legault, B., and Rodriguez-Valera, F. (2005) *Proc. Natl. Acad. Sci. U. S. A.* **102,** 18147–18152

24. Marmur, J. (1961) *J. Mol. Biol.* **3,** 208–218

25. Kandori, H., Shimono, K., Sudo, Y., Iwamoto, M., Shichida, Y., and Kamo, N. (2001) *Biochemistry* **40,** 9238–9246

26. Iwata, T., Nozaki, D., Tokutomi, S., Kagawa, T., Wada, M., and Kandori, H. (2003) *Biochemistry* **42,** 8183–8191

27. Shimono, K., Ikeura, Y., Sudo, Y., Iwamoto, M., and Kamo, N. (2001) *Biochim. Biophys. Acta* **1515,** 92–100

28. Spudich, J. L. (2006) *Trends Microbiol.* **14,** 480–487

29. Yao, V. J., and Spudich, J. L. (1992) *Proc. Natl. Acad. Sci. U. S. A.* **89,** 11915–11919

30. Olson, K. D., Zhang, X. N., and Spudich, J. L. (1995) *Proc. Natl. Acad. Sci. U. S. A.* **92,** 3185–3189

31. Zhang, X. N., and Spudich, J. L. (1997) *Biophys. J.* **73,** 1516–1523

32. Jung, K. H., and Spudich, J. L. (1998) *J. Bacteriol.* **180,** 2033–2042

33. Sasaki, J., Phillips, B. J., Chen, X., Van Eps, N., Tsai, A. L., Hubbell, W. L., and Spudich, J. L. (2007) *Biophys. J.* **92,** 4045–4053

34. Seidel, R., Scharf, B., Gautel, M., Kleine, K., Oesterhelt, D., and Engelhard, M. (1995) *Proc. Natl. Acad. Sci. U. S. A.* **92,** 3036–3040

35. Balashov, S. P., Imasheva, E. S., Boichenko, V. A., Anton, J., Wang, J. M., and Lanyi, J. K. (2005) *Science* **309,** 2061–2064

36. Takahashi, T., Yan, B., Mazur, P., Derguini, F., Nakanishi, K., and Spudich, J. L. (1990) *Biochemistry* **29,** 8467–8474

37. Shimono, K., Hayashi, T., Ikeura, Y., Sudo, Y., Iwamoto, M., and Kamo, N.

(2003) *J. Biol. Chem.* **278,** 23882–23889

38. Pettei, M. J., Yudd, A. P., Nakanishi, K., Henselman, R., and Stoeckenius, W. (1977) *Biochemistry* **16,** 1955–1959

39. Kamo, N., Hazemoto, N., Kobatake, Y., and Mukohata, Y. (1985) *Arch. Biochem. Biophys.* **238,** 90–96

40. Imamoto, Y., Shichida, Y., Hirayama, J., Tomioka, H., Kamo, N., and Yoshizawa, T. (1992) *Biochemistry* **31,** 2523–2528

41. Scharf, B., Hess, B., and Engelhard, M. (1992) *Biochemistry* **31,** 12486–12492

42. Olson, K. D., Deval, P., and Spudich, J. L. (1992) *Photochem. Photobiol.* **56,** 1181–1187

43. Sudo, Y., Iwamoto, M., Shimono, K., and Kamo, N. (2002) *Biophys. J.* **83,** 427–432

44. Spudich, J. L. (1995) *Biophys. Chem.* **56,** 165–169

45. Sudo, Y., Iwamoto, M., Shimono, K., Sumi, M., and Kamo, N. (2001) *Biophys. J.* **80,** 916–922

46. Spudich, J. L., and Lanyi, J. K. (1996) *Curr. Opin. Cell Biol.* **8,** 452–457

47. Sudo, Y., and Spudich, J. L. (2006) *Proc. Natl. Acad. Sci. U. S. A.* **103,** 16129–16134

48. Tsuda, M., Hazemoto, N., Kondo, M., Kamo, N., Kobatake, Y., and Terayama, Y. (1982) *Biochem. Biophys. Res. Commun.* **108,** 970–976

49. Hazemoto, N., Kamo, N., Terayama, Y., Kobatake, Y., and Tsuda, M. (1983) *Biophys. J.* **44,** 59–64

50. Bogomolni, R. A., and Spudich, J. L. (1982) *Proc. Natl. Acad. Sci. U. S. A.* **79,** 6250–6254

51. Spudich, E. N., and Spudich, J. L. (1982) *Proc. Natl. Acad. Sci. U. S. A.* **79,** 4308–4312

52. Pebay-Peyroula, E., Rummel, G., Rosenbusch, J. P., and Landau, E. M. (1997) *Science* **277,** 1676–1681

53. Luecke, H., Schobert, B., Richter, H. T., Cartailler, J. P., and Lanyi, J. K. (1999) *J. Mol. Biol.* **291,** 899–911

54. Luecke, H., Schobert, B., Lanyi, J. K., Spudich, E. N., and Spudich, J. L. (2001) *Science* **293,** 1499–1503

55. Gordeliy, V. I., Labahn, J., Moukhametzianov, R., Efremov, R., Granzin, J., Schlesinger, R., Buldt, G., Savopol, T., Scheidig, A. J., Klare, J. P., and Engelhard, M. (2002) *Nature* **419,** 484–487

56. Moukhametzianov, R., Klare, J. P., Efremov, R., Baeken, C., Goppner, A., Labahn, J., Engelhard, M., Buldt, G., and Gordeliy, V. I. (2006) *Nature* **440,** 115–119